Early detection of cell activation events by means of attenuated total reflection Fourier transform infrared spectroscopy

Jitto Titus, Chadi Filfili, Julia K. Hilliard, John A. Ward, and A. G. Unil Perera

Citation: Applied Physics Letters **104**, 243705 (2014); doi: 10.1063/1.4885081
View online: http://dx.doi.org/10.1063/1.4885081
View Table of Contents: http://scitation.aip.org/content/aip/journal/apl/104/24?ver=pdfcov
Published by the AIP Publishing

Early detection of cell activation events by means of attenuated total reflection Fourier transform infrared spectroscopy

Jitto Titus,[1,a)] Chadi Filfili,[2,a)] Julia K. Hilliard,[2] John A. Ward,[3] and A. G. Unil Perera[1,b)]
[1]*Optoelectronics Laboratory, Department of Physics and Astronomy, GSU, Atlanta, Georgia 30303, USA*
[2]*Viral Immunology Center, Department of Biology, GSU, Atlanta, Georgia 30303, USA*
[3]*Department of Clinical Investigation, Brooke Army Medical Center, Fort Sam Houston, San Antonio, Texas 78234, USA*

(Received 16 December 2013; accepted 13 June 2014; published online 20 June 2014)

Activation of Jurkat T-cells in culture following treatment with anti-CD3 (Cluster of Differentiation 3) antibody is detectable by interrogating the treated T-cells using the Attenuated Total Reflection–Fourier Transform Infrared (ATR-FTIR) Spectroscopy technique. Cell activation was detected within 75 min after the cells encountered specific immunoglobulin molecules. Spectral markers noted following ligation of the CD3 receptor with anti CD3 antibody provides proof-of-concept that ATR-FTIR spectroscopy is a sensitive measure of molecular events subsequent to cells interacting with anti-CD3 Immunoglobulin G. The resultant ligation of the CD3 receptor results in the initiation of well defined, specific signaling pathways that parallel the measurable molecular events detected using ATR-FTIR. Paired t-test with *post-hoc* Bonferroni corrections for multiple comparisons has resulted in the identification of statistically significant spectral markers ($p < 0.02$) at 1367 and 1358 cm^{-1}. Together, these data demonstrate that early treatment-specific cellular events can be measured by ATR-FTIR and that this technique can be used to identify specific agents via the responses of the cell biosensor at different time points postexposure. © *2014 AIP Publishing LLC*. [http://dx.doi.org/10.1063/1.4885081]

The application of infrared spectroscopy to measure and identify cellular responses has numerous benefits.[1–3] Cells in culture mount stimulus-specific responses that are induced by receptor:ligand interactions. Here, it is hypothesized that attenuated total reflection–Fourier transform infrared (ATR-FTIR)[4] can be used to identify ligands, e.g., antibodies, pathogens, allergens, molecules, which interact with cells in culture initially via cell surface receptors. The cell under these conditions serves as a "sensor"[5] of the surrounding microenvironment. The identification of the ligand(s) is accomplished by analysis of the resultant ATR-FTIR read-out of ligand-induced perturbations in the cell "sensor," which initiate intracellular signaling pathways activated as a result of the cell:ligand interactions. Ligands can also be viruses as these interact with specific receptors on the surfaces of cells resulting in types of cytopathic changes over time. These changes have been used historically to identify the presence of viruses in clinical samples, but days and even weeks are sometimes required. Confirmatory assays for specific pathogen identification currently depend on complex molecular methods and the use of defined biological and chemical probes. These assays are generally elaborate and require specific reagents as well as highly trained technologists and considerable time ranging from 3 h (Ref. 6) to weeks where there is sufficient material for detection. On the other hand, cellular responses become engaged immediately after a cell detects a foreign agent, a stimulant, an antibody, or a pathogen. Learning how to interrogate cells exposed to foreign agents can provide a rapid and sensitive means to identify agents, circumventing the need for more time consuming, technologically complex testing. ATR-FTIR, one mechanism by which cells can be interrogated, greatly reduces background noise, and is more sensitive to the events occurring on the cell membrane compared to transmission FTIR because the interrogating light penetrates only about 2 μm into the cell suspension rather than the entire thickness of the cell suspension spot as in transmission FTIR. The ATR-FTIR configuration also produces enhanced resolution of spectral features.[7] This is confirmed by the features seen in Fig. 1, inset (b), where more details with greater signal-to-noise ratios are visible in the ATR-FTIR absorbance curve compared to the FTIR absorbance curve. The use of FTIR Spectroscopy is reported, employing the ATR technique to detect early activation events in Jurkat T-cells after ligation of cell surface cluster of differentiation 3 (CD3)-receptors by a specific antibody (anti-CD3) at 75 min post-treatment. These findings serve as proof-of-concept that cells in culture can be used as sensors to specifically and rapidly probe the surrounding microenvironment. These sensors generate specific spectral patterns resulting from activation of signaling pathways that can serve to identify the specific ligand:receptor interactions, which result in a series of intracellular activities over time. ATR-FTIR can interrogate these cells at time points as early as 5 min postexposure/stimulation, or approximately the time it takes the cells to settle onto the crystal surface.

Inset (a) of Fig. 1 is a schematic of the ATR technique where a mid-infrared light beam passes through a Zinc Selenide (ZnSe) crystal such that it is totally internally reflected creating an evanescent wave penetrating ~2 μm into the cell suspension deposited on the ZnSe crystal. The

[a)]J. Titus and C. Filfili contributed equally to this work.
[b)]E-mail: uperera@gsu.edu

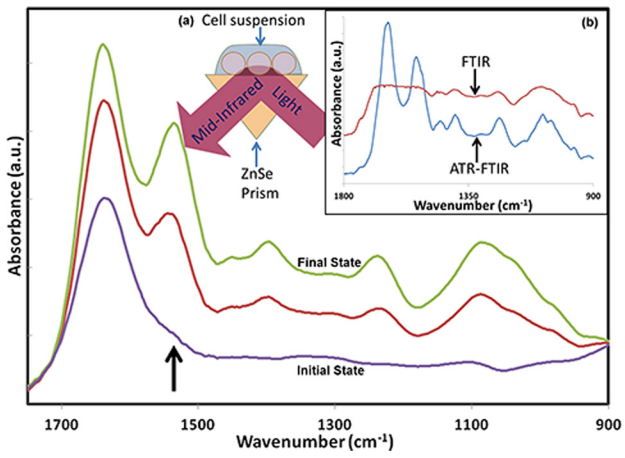

FIG. 1. ATR-FTIR spectra of Jurkat cells in culture medium initially showing the characteristic peaks of the medium and ~15 min later the peaks representative of the Jurkat cells along with the medium. For example, the arrow indicates the frequency at which the absorption corresponding to Amide II occurs, which is characteristic of cells as they settle.

light is absorbed by the cell suspension as dictated by the vibrational modes of the components. (The penetration depth and size of the cells are enlarged for clarity.)

Inset (b) of Fig. 1 shows the spectra obtained by the conventional transmission mode FTIR and the ATR-FTIR spectroscopy. The ATR-FTIR spectra shows higher signal to noise ratio and better resolved peaks than observed with transmission FTIR alone.

When electromagnetic radiation passes through a material, photons of certain frequencies of light, whose energies correspond to the vibrational frequencies of atomic and molecular bonds are absorbed. ATR is a particular configuration where light is totally internally reflected inside a prism of high refractive index (Fig. 1, inset (a)). Some photons penetrate out of the surface of the crystal and then are coupled back in. This evanescent wave interacts with any material on the surface of the crystal, and thus, the intensities of the frequencies of light measured after passing through the prism are highly sensitive to the materials present on the surface of the crystal.

Jurkat T-cells[8] were chosen as model biosensors to be interrogated using the ATR-FTIR spectroscopic technique. Jurkat cells, clone E6-1 (ATCC # TIB-152) were grown in log-phase in R-10 growth medium (RPMI-1640, (Mediatech Manassas, VA); supplemented with 10% fetal bovine serum (FBS), 100 U/ml penicillin, and 100 μg/ml streptomycin). Cells were counted and checked for viability by the trypan blue exclusion method and only cells with >95% viability were accepted as sensors. The cells were then aliquoted into approximately 1×10^6 cells each in sterile capped 1.5 ml vials, and centrifuged at room temperature for 4 min at 800 g. The growth medium was then completely removed and replaced with 100 μl of either fresh R-10, a matched isotype control antibody, or with R-10 supplemented with 100 ng/ml anti-CD3 Immunoglobulin G (IgG) (Mabtech, Nacka Strand, Sweden). Cells were gently mixed and incubated in a humidified chamber at 37 °C in 5% CO_2 for 75 min with the vial lids loosened to allow for gas exchange. At the end of the incubation, the contents of two vials with the same treatment conditions were then pooled together (2×10^6 cells per vial). Ice-cold unsupplemented RPMI-1640 medium (1 ml) was added to each vial, which was then centrifuged at 800 g for 4 min at room temperature. The supernatant was removed and the pellet washed a second time with 1 ml of ice-cold unsupplemented RPMI-1640 medium after which the supernatant was removed completely. The pellet of 2×10^6 cells was re-suspended in 16 μl of cold, fresh, unsupplemented RPMI-1640 medium, placed on ice and transported to the FTIR laboratory for ATR/FTIR analysis (~10 min).

Jurkat cells without the anti-CD3 IgG treatment or with an equivalent amount of isotype IgG were used as negative controls. The activated state of the experimentally treated cells and the unactivated state of the control cells were validated with parallel flow cytometry experiments (Fig. 2) to measure cell surface expression of the activation marker CD69. The presence of this marker was measured at 24 h postactivation by probing the cell surface (30 min, on ice) with CD69 (Fluorescein isothiocyanate) FITC-conjugated antibody (BD Biosciences, San Jose, CA) per manufacturer instructions and measured on a BD LSR Fortessa flow cytometer (BD BioSciences, San Jose, CA).

For ATR-FTIR analysis, 5 μl aliquots of cell suspension (~625 000 cells) were spotted on ZnSe ATR crystal of the Bruker Vertex 70 FTIR spectrometer and allowed to air dry. Spectral data were collected in the range of 1500–800 cm^{-1} for the activated and unactivated cells with a spectral resolution of 4 cm^{-1}. As the water evaporated once cells were deposited (~15 min), the cells settled to the surface of the crystal and spectral peaks indicative of the biological materials of the cells, e.g., proteins, DNA, and phospholipids in addition to that of the medium were captured. Each one of the 11 independently prepared activated and unactivated cell sets was scanned by ATR five times consecutively, where each scan consisted of a co-added average of 50 scans.

Sharp spikes due to moisture were evident in the spectral range of 1500–1300 cm^{-1} arising from the standard

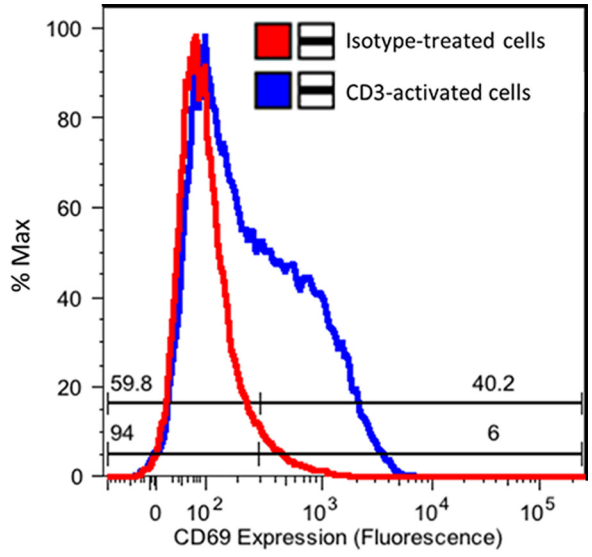

FIG. 2. CD69 expression 1 day postactivation in CD3-activated Jurkat cells compared to an antibody isotype treated control. This is representative of flow cytometric confirmation of cell activation in our experimental set up that repeatedly yielded >30% increase in CD69 expression after 24 h.

background subtraction process of the OPUS 6.5 software (Bruker Optics). These spikes were due to the differing moisture levels in the sample chamber during the collection of the background spectrum compared to the sample spectrum resulting in either peaks or dips. These artifacts were corrected by using an absorbance spectrum of just moisture collected concurrently during sample measurement. In later experiments, the moisture noise was further reduced by employing an ATR with dry air purging capability; these experiments also confirmed the tenability of the moisture compensation process. A five point moving average was performed and the spectrum was vector normalized using OPUS 6.5, where the average of all the absorbance values of the spectrum was subtracted from the entire spectrum. This reduced the mid-spectrum to zero. Then the sum of the squares of all the absorbance values was calculated and the spectrum divided by the square root of this sum. The vector normalized ATR spectra revealed some marked differences between the activated and unactivated cells (Fig. 3).

Specific frequencies at which the absorbance varied between the activated and the unactivated cells were identified by visual observations. Four spectral frequencies, namely, 1358, 1367, 1335, and 1250 cm^{-1} were selected[9] and the differences between the absorbances at these identified frequencies were considered as the differentiating markers. At 1358 cm^{-1} CH_2-CH rocking shifts are measured.[10,11] These shifts are predicted to occur with perturbations to the lipid bilayer comprising the cell membrane. Additionally, protein phosphorylation at specific amino acid residues will alter these bonds. Changes near wavenumber 1367 cm^{-1} arise from deformation[11] of CH_3-, which again reflects membrane changes, likely mirroring events occurring around intracellular membranes, e.g., perturbations in the plasma membranes, nuclear membranes, and endoplasmic reticulum during binding of adapter molecules to the cytoplasmic domain of CD3, resultant signaling, and ultimately nuclear translocation events.

The other significant changes at 1335 cm^{-1} are associated with wagging[10] shifts of CH_2-CH. Such shifts predictably occur with modifications, e.g., post-translational modifications, dimerization reflecting protein:protein interactions, while 1250 cm^{-1} measures carbon lattice perturbations.[10] Membrane perturbations will predictably be associated with these events.

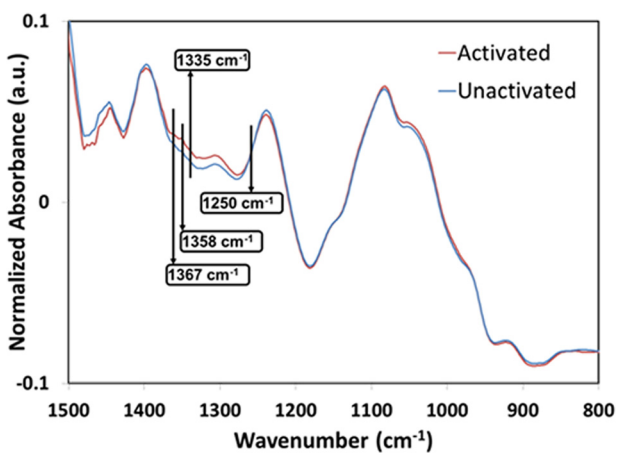

FIG. 3. The ATR spectra of the activated and unactivated cells indicating spectral markers with absorbance values that differentiate activated from unactivated cells. The markers are: 1367 cm^{-1}(CH_3- deformation) 1358 cm^{-1} (CH_2-CH rocking), 1335 cm^{-1} (CH_2-CH wagging), and 1250 cm^{-1} (Carbon lattice perturbations, Amide III of proteins).

The null hypothesis states that there will be no difference in the ATR spectrum of Jurkat cells as a function of their state of activation: stimulated with anti-CD3 antibody versus unstimulated. The alternative hypothesis states that there will be differences in the ATR spectrum as a function of the state of stimulation. The independent or predictor variables were the state of activation and the dependent variables were spectral absorbance values.

A two-tailed paired student's t-test was performed using Microsoft Excel 2010 on the absorbance values at the chosen markers and was followed by *post-hoc* Bonferroni corrections for multiple comparisons with false discovery rate analysis. A confidence interval of 95% was chosen as a test of significance. Of the four spectral markers (Table I), the differences at 1358 cm^{-1} and 1367 cm^{-1} efficiently distinguished the activated from the unactivated cells at 75 min after cell incubation with anti-CD3 antibody in eleven independent experiments with p-values of 0.02. Thus, the null hypothesis is rejected and the alternate hypothesis is accepted. The markers at 1335 cm^{-1} and 1250 cm^{-1} have p values of 0.028 and 0.038, respectively.

ATR-FTIR spectroscopic tool has been effectively used here to rapidly detect Jurkat cells early activation events mediated by exposure of cells to antibody specific to the CD3 T-cell coreceptor. Cells were interrogated 75 min post-exposure and the ratios of specific absorbance values of the cells were calculated and used to differentiate treatment groups. Research is currently underway to study the efficacy of using ATR-FTIR spectral markers to identify and differentiate specific agents to which the cells were exposed. In these experiments, we have validated that the treatment conditions mediate T-cell activation determined by CD 69 cell surface expression. Fig. 2 shows a representative output of the validation experiment. An approximate 30% increase in CD69 expression was observed confirming that cells were in fact activated as compared to the isotype treated controls. Ligation of the T-cell receptor, which occurs by treatment of the cells with anti-CD3 activates T cells by modulating specific molecular events including the assembly of specific activation complexes that initiate after the recruitment of the molecule ZAP-70[12,13] (Zeta-chain-associated protein kinase 70) to the cytoplasmic domain of ligated CD3. Ultimately, experimental correlation of the spectral changes with specific activation of signaling events induced by specific agents using more directed approaches will enhance our understanding of the relationship between spectral changes and recruitment of specific molecular interactions.

The spectral changes reported in this work are consistent over numerous experiments, however, the association of these spectral changes with specific molecular events requires additional experimentation to identify whether specific molecular interactions have cause and effect relationships or are simply correlative, non-causal events induced by the cells that are interacting with specific molecules or pathogens, especially because hundreds of genes can be modulated within 2 h of early activation events.[14] To identify

TABLE I. Paired t-tests on selected spectral bands, corrected for multiple comparisons with false discovery rate analysis.

Comparisons	Wavenumber (cm^{-1})	Paired t-test Significance	*Post-hoc* Bonferroni correction	Statistically significant?
1	1358	0.020	0.050	Yes
2	1367	0.020	0.025	Yes
3	1335	0.028	0.017	No
4	1250	0.038	0.013	No

specific interactions resulting from interactions of cells with agents within the immediate microenvironment, this experimental model was developed to tightly control the cell membrane and subsequent cytoplasmic events stimulated by the initial interaction, optimizing the technical conditions that enable rapid, efficient, and consistent interrogation of the cell biosensor. The cell as a biosensor responds to cell surface interactions by initiating intracellular signaling pathways that are well defined. These signaling pathways are unique for specific cellular receptors following ligand interaction, e.g., the Type-1 interferon receptor ligated to Type 1 interferon or an agonist, which results in intracellular interactions with the cytoplasmic domains of the receptor and Janus kinase (JAK) proteins that are phosphorylated to the cytoplasmic portions of the surface receptor.[15,16] The JAK proteins subsequently recruit STAT-1 (Signal Transducers and Activators of Transcription) proteins, which are phosphorylated subsequently. The series of kinase, phosphate, and protein:protein interactions continue until transcription factors dimerize and translocate to the nucleus[17] to bind to the promoter that drive the genes under the control of the specific receptor that begins the entire sequence of events.[18] ATR-FTIR is then excellent for interrogating modifications and protein interactions occurring in the pathways, along with the protein:DNA interactions, and the subsequent mRNA synthesis.[19] The temporal progression of these events may or not be causal of specific spectral changes measured at the time of ATR-FTIR interrogation, however, these events are occurring and contribute to the overall changes in the cell postexposure. The identified spectral markers will be common only to ligands that interact in precisely the same manner with the CD3 receptor, thus, this technique can be exploited to identify a specific combination of spectral markers at activation time points that are unique to the activating interactions induced by a specific receptor:ligand coupling.

The utility of using this relatively simple and direct detection of protein modifications, protein:protein interactions, protein:DNA binding, and synthesis of new mRNA transcripts, each resulting in spectral perturbations and the applicability of these measurements to pathogen detection with cells serving as biosensors provides a unique and reliable system for rapid identification of noxious agents and pathogens that threaten health and wellbeing. Cells within organisms are the most sensitive detectors known, far surpassing current technology. Thus, exploiting these as microlaboratories to procure readouts indicative of agents interacting with these sensors has the ability to take detection technologies to the next level.

This work was supported in part by the Molecular Basis of Disease Area of Focus, Georgia State University, Atlanta, GA 30303, Georgia Research Alliance, AFOSR: 55655-EL-DURIP and DOD: W81XWH-06-1-0795.

[1]V. Erukhimovitch, M. Talyshinsky, Y. Souprun, and M. Huleihel, *DNA Viruses* (Springer, 2005), pp. 161–172.
[2]G. Hastings, P. Krug, R. L. Wang, J. Guo, H. P. Lamichhane, T. Tang, Y. S. Hsu, J. Ward, D. Katz, and J. Hilliard, Analyst **134**(7), 1462–1471 (2009).
[3]F. T. Lee-Montiel, K. A. Reynolds, and M. R. Riley, J. Biol. Eng. **5**, 16 (2011).
[4]S. G. Kazarian and K. L. Chan, Analyst **138**(7), 1940–1951 (2013).
[5]J. Hilliard, C. Filfili, I. Patrusheva, P. Fuchs, D. Katz, R. Wang, G. Hastings, M. J. Guo, Y.-S. Hsu, and J. Ward, in *Use of Advanced Technologies and New Procedures in Medical Field Operations*, edited by N. Sto (Essen, Germany, 2010), p. 29.
[6]V. Erukhimovitch, E. Bogomolny, M. Huleihil, and M. Huleihel, Analyst **136**(13), 2818–2824 (2011).
[7]C. S. Ng, H. Kato, and T. Fujita, Int. Immunol. **24**(12), 739–749 (2012).
[8]W. F. Hawse, M. M. Champion, M. V. Joyce, L. M. Hellman, M. Hossain, V. Ryan, B. G. Pierce, Z. Weng, and B. M. Baker, J. Immunol. **188**(12), 5819–5823 (2012).
[9]W. Urbaniak-Domagala, in *Advanced Aspects of Spectroscopy*, edited by M. A. Farrukh (InTech, 2012).
[10]Z. Movasaghi, S. Rehman, and I. U. Rehman, Appl. Spectrosc. Rev. **43**(2), 134–179 (2008).
[11]A. Bright, T. Renuga Devi, and S. Gunasekaran, Int. J. ChemTech Res. **2**(1), 379–388 (2010).
[12]L. Barboza, S. Salmen, G. Teran-Angel, D. L. Peterson, and L. Berrueta, Cell. Immunol. **284**(1–2), 9–19 (2013).
[13]H. Wang, T. A. Kadlecek, B. B. Au-Yeung, H. E. Goodfellow, L. Y. Hsu, T. S. Freedman, and A. Weiss, Cold Spring Harbor Perspect. Biol. **2**(5), a002279 (2010).
[14]C. Cheadle, J. Fan, Y. S. Cho-Chung, T. Werner, J. Ray, L. Do, M. Gorospe, and K. G. Becker, BMC Genomics **6**, 75 (2005).
[15]N. A. de Weerd, S. A. Samarajiwa, and P. J. Hertzog, J. Biol. Chem. **282**(28), 20053–20057 (2007).
[16]A. Borroto, I. Arellano, R. Blanco, M. Fuentes, A. Orfao, E. P. Dopfer, M. Prouza, M. Suchanek, W. W. Schamel, and B. Alarcon, J. Immunol. **192**(5), 2042–2053 (2014).
[17]R. Wang, P. Cherukuri, and J. Luo, J. Biol. Chem. **280**(12), 11528–11534 (2005).
[18]D. Hebenstreit, J. Horejs-Hoeck, and A. Duschl, Drug News Perspect. **18**(4), 243–249 (2005).
[19]S. G. Kazarian and K. L. A. Chan, Biochim. Biophys. Acta, Biomembr. **1758**(7), 858–867 (2006).